HTML ABSTRACT + LINKS

Interstitial charge states in boron-implanted silicon

M. Y. L. Jung, Charlotte T. M. Kwok, Richard D. Braatz, and E. G. Seebauer[a)]
Department of Chemical Engineering, University of Illinois, Urbana, Illinois 61801

(Received 14 June 2004; accepted 13 October 2004; published online 11 March 2005)

It is becoming increasingly clear that simulation models of transient enhanced diffusion (TED) in silicon need to incorporate interstitial charging effects accurately in order to adequately reproduce experimental data near the surface and near the underlying junction. However, in the case of boron TED, the relevant charge states and ionization levels of both boron and silicon interstitial atoms are known only imperfectly. The present work attempts to describe this behavior more accurately via simulations of implanted profiles that employ a model whose kinetic parameters have been determined with considerable confidence by rigorous systems methods. The results suggest that B has two relevant charge states: (+) and (−). The corresponding states for Si are (++) and (0). The effective ionization levels for B and Si are 0.33 ± 0.05 and 0.12 ± 0.05 eV above the valence band maximum, respectively. © *2005 American Institute of Physics*. [DOI: 10.1063/1.1829787]

I. INTRODUCTION

Transient enhanced diffusion (TED) of ion-implanted dopants in silicon has attracted a great deal of study over the last three decades[1–4] because TED plays a significant role in limiting the shallowness of *pn* transistor junctions in advanced microelectronic devices.[5] Interstitial atoms generated by implantation serve as the primary mediators of TED. Trapping or absorption of these interstitials by larger defects such as dislocation loops, interstitial clusters, and nearby surfaces or interfaces is well known to affect the magnitude of TED and the shape of the resulting dopant profile.

However, it is becoming increasingly clear that simulation models of TED also need to incorporate interstitial charging effects accurately in order to adequately reproduce experimental data, especially near the surface and near the underlying junction. For example, electric fields associated with band bending near atomically clean Si surfaces[6] and $Si-SiO_2$ interfaces after implantation[7] can interact with charged interstitials to transform the boundary from a significant sink into a good reflector, which has the net effect of deepening the underlying junction.[7,8] Band bending also provides a mechanism for dopant pileup near the boundary if boron interstitials can assume a negative charge[8] and if the associated ionization level is below roughly midgap. Up to now, simulators have proven inadequate for even qualitative predictions of this phenomenon.[9] As junction depths become progressively shallower because of device scaling, the importance of surfaces and interfaces in controlling such phenomena becomes correspondingly greater. Down near the junction, the built-in electric fields can also interact with charged interstitials to affect their motion[10,11] and consequently the junction depth and profile steepness.

However, for boron TED, the relevant charge states and ionization levels of both boron and silicon interstitial atoms are known only imperfectly. This laboratory has recently developed a model for dopant diffusion and activation based on rigorous systems-based analysis.[12–16] The present work employs profile simulations using that model to describe charging behavior more accurately. The results suggest that B has two relevant charge states: (+) and (−). The corresponding states for Si are (++) and (0). The effective ionization levels for B and Si are 0.33 ± 0.05 and 0.12 ± 0.05 eV above the valence band maximum, respectively.

II. MODEL

A. Simulation method

Calculations were performed using the profile simulator FLOOPS 2000 (by Mark E. Law of the University of Florida and Al Tasch of the University of Texas/Austin)[17] with kinetic rate expressions and parameters reported in Ref. 16. No-flux boundary conditions were employed for interstitials at the surface. Simulation results were compared to data from secondary ion mass spectroscopy (SIMS) reported previously[16] for Si wafers implanted with B at 0.60 keV with a fluence of 2×10^{15} ions/cm^2 at 0° tilt. The heating program was a conventional "spike anneal" described in Ref. 16, with heating rates varying from 75 to 350 °C/s. Diffusivities for the interstitials were assumed to be independent of charge state. As discussed elsewhere,[12] the literature does not provide a sufficient basis for assigning a charge state dependence to these diffusivities, although such dependence may exist. Fortunately, formal parameter sensitivity analysis has shown that the diffusivity of Si interstitials plays essentially no role in affecting junction depth or dopant activation.[14] On the other hand, the diffusivity of B interstitials does play a significant role. The present simulations suggest, however, that this diffusivity takes a back set to charge state in determining the most important metric of profile shape examined here: the slope of the profile near the junction.

Some explanation is in order to clarify the relationship between the rate parameters of Ref. 16 and those determined here. The activation energies of Ref. 16 were obtained by integrating literature values together with experimental dopant profiles measured by SIMS. The integration was accomplished using systems-based mathematical methods, begin-

[a)]Author to whom correspondence should be addressed; electronic mail: eseebaue@uiuc.edu

 © 2005 American Institute of Physics

Downloaded 07 Aug 2007 to 130.126.226.215. Redistribution subject to AIP license or copyright, see http://jap.aip.org/jap/copyright.jsp

ning with the maximum likelihood estimation to develop an optimally likely parameter set from the totality of literature reports. This parameter set was then refined using SIMS data together with maximum *a posteriori* (MAP) estimation. MAP accomplished the refining by solving a global optimization problem employing both simulation results and experimental profiles. However, the simulations used existing literature to assume a set of values for the charges in the interstitials [(+) and (−) for B, and (++), and (0) for Si] as well as ionization levels for those charge states roughly equivalent to those determined here. As will be discussed later, literature reports for the identities and ionization levels of the charge states are far from conclusive. The simulations described here seek to verify and refine the assumed values for these quantities based on the parameter set that emerged from MAP analysis.

There is no tautology in this verification and refining, however, because the parameters emerging from MAP analysis depended upon a global optimization procedure using the entire profile, whereas the present comparison between simulation and experiment focuses upon qualitative comparison primarily of profile slopes near the junctions and secondarily of junction depth. Thus, the uses of the experimental data differ significantly enough to be considered independent of each other.

B. Charge statistics

To solve Eqs. (1)–(3) for the mobile species requires that assumptions be made regarding charge states available to these species as well as their "ionization levels"—values of the Fermi energy at which the majority charge state changes. Since neither the stable charge states nor the ionization levels are definitively known for the key species B_i and Si_i, this work seeks to determine these properties by comparing simulations based upon a variety of assumed properties with experimental B profiles determined by SIMS. To narrow the likely range of parameters, however, we relied to a significant extent on the knowledge already available in the literature.

There exists significant experimental and computational evidence that charge states for interstitial boron in *p*-type Si below room temperature are B_i^+ and B_i^-. Experimentally, Harris *et al.*[18] interpreted photogenerated signals from deep level transient spectroscopy and electron paramagnetic resonance in the range 50–250 K in terms of a donor (+/0) level close to the conduction band minimum E_c at $E_c-0.13$ eV and a lower-lying acceptor level (0/−) at $E_c-0.45$ eV. These results correspond to "negative-*U*" behavior in which one ionization event leads quickly to a second, in this case destabilizing the neutral state with respect to the positive and negative. Computations by the density functional theory (DFT) largely confirm this finding,[19] indicating that B_i converts from a positively charged split (or possibly tetrahedral) configuration to a negatively charged hexagonal configuration at $E_v+0.27$ eV. In this vicinity, however, the calculations also predicted neutral split and hexagonal states with formation energies only slightly higher (~0.1 eV) than the charged states. Given the significant uncertainties associated with the DFT computations of this sort, the neutral states cannot be ruled out.

Furthermore, these combined results do not preclude the dominance of B_i^0 at higher temperatures. Indeed, the ionization levels associated with the pertinent charge states can move significantly as temperature rises and the band gap shrinks. Ionization levels for donors tend to track the valence band as the band gap shrinks, while the levels for acceptors track the conduction band. Such phenomena are associated with the ionization entropy of point defects as first described for bulk defects in Si[20,21] and later for the corresponding surface defects.[22] Indeed, Haller *et al.*[23] and Uematsu[24] have satisfactorily modeled diffusion data for boron using the neutral state.

For Si interstitials, the most likely charge states in *p*-type Si are also incompletely established. The possible candidates[19,25–29] include Si_i^{++}, Si_i^0, Si_i^-, and Si_i^{--}.[25] Fair[11] employed Si_i^+ and Si_i^0 to rationalize the shapes of TED profiles for implanted boron, but subsequent computational work by the DFT and related methods suggested that Si_i^+ is destabilized by negative-*U* behavior[25,28,29] at 0 K. Thus, doubt was cast upon the interpretation of the TED data, but again the temperature regimes were sufficiently different to leave open the possibility that Si_i^+ plays a role under processing conditions.

For Si_i, no experimental work exists concerning ionization levels. Computational results from Lee *et al.*,[25] Harrison,[28] and Zhu[29] based on the DFT suggest that the ionization levels differ considerably for the three different site configurations available to Si_i. Lee *et al.* reported that the lowest energy state is Si_i^{++} in the tetrahedral configuration below $E_v+0.73$ eV, with a switch to Si_i^- in the [110]-split configuration at higher Fermi energies. Hakala *et al.*[19] found the same configurations, but the charge state switches instead from Si_i^{++} to Si_i^0 at $E_v+0.62$ eV. (This value was calculated from the data in their Table II.) The corresponding value from Zhu's DFT calculations is $E_v+0.45$ eV.[29] (Harrison[28] used a semianalytical approach that assumes this switch occurs at the middle of the band gap, or $E_v+0.6$ eV at 0 K.) Lee *et al.*[25] reported a further switch to Si_i^{--} in the [110]-split configuration above $E_v+1.02$ eV, while Zhu found a switch to Si_i^- at $E_v+1.01$ eV.

Clearly there exists much disagreement about the existence and nature of negative charge states in strongly *n*-doped Si. However, for *p*-type and weakly *n*-type material, the preponderance of evidence points to the Si_i^{++} and Si_i^0 states as most important, with an arithmetically averaged ionization level at $E_v+0.54$ eV. During high-temperature diffusion, however, several geometric configurations are probably sampled—not all of them having the lowest energy. The appropriate effective ionization level $E_{Si i}*$ to use for the (++/0) transition therefore becomes unclear.

Given this uncertain state of affairs for both B_i and Si_i, we fitted experimental TED profiles using several plausible combinations of charge states, using the effective ionization levels $E_{Bi}*$ and $E_{Si i}*$ as adjustable parameters.

For computational tractability, the mass balance equations of Eq. (1) were set up to track the total concentration of

Downloaded 07 Aug 2007 to 130.126.226.215. Redistribution subject to AIP license or copyright, see http://jap.aip.org/jap/copyright.jsp

each type of defect (including all charge states) rather than each charge state. Such an approach requires the assumption that defects reach their thermodynamically appropriate charge states on a time scale that is fast compared with defect motion and reaction. This assumption has long been employed in the modeling of defects in Si, for example in diffusion by the Bourgoin mechanism[30] wherein charge state changes even during the course of an individual diffusive hop. To give a specific example of how the mass balance equations were formulated, we take the case of interstitial boron, assumed to exist as B_i^+ and B_i^- species. The transient mass balance for total B_i becomes

$$\frac{\partial B_i}{\partial t} = \frac{\partial B_i^+}{\partial t} + \frac{\partial B_i^-}{\partial t}. \tag{1}$$

Assuming that the intrinsic diffusivities of B_i^+ and B_i^- are equal, Eq. (1) can be combined with basic mass balance equations based on Fick's second law to become

$$\frac{\partial B_i}{\partial t} = D_{B_i}\left\{\frac{\partial^2 B_i}{\partial x^2} + \frac{1}{\alpha}\left[\gamma_B B_i \frac{\partial^2 \psi}{\partial x^2} + \frac{\partial \psi}{\partial x}\frac{\partial}{\partial x}(\gamma_{B_i} B_i)\right]\right\} + G_{B_i}, \tag{2}$$

where G denotes a net generation rate. The parameter $\alpha = kT/q$, with k being Boltzmann's constant, T being temperature, and q the electron charge. The parameter γ_{Bi} obeys

$$\gamma_{B_i} = \gamma_{B_i^+} - \gamma_{B_i^-} \tag{3a}$$

$$\text{with } \gamma_{B_i^-} = \frac{B_i^-}{B_i} = \left[1 + \frac{1}{g}\exp\left(\frac{E_{B_i^-} - E_F}{kT}\right)\right]^{-1} \tag{3b}$$

$$\text{and } \gamma_{B_i^+} = \frac{B_i^+}{B_i} = \left[1 + g\exp\left(\frac{E_F - E_{B_i^+}}{kT}\right)\right]^{-1}. \tag{3c}$$

The parameters $\gamma_{B_i^+}$ and $\gamma_{B_i^-}$ represent the relative fractions of interstitial boron in the positive and negative states, respectively. The degeneracy factor g[21,31] in Eqs. (3b) and (3c) equals unity for the interstitial pair B_i^+ and B_i^- (as well as for Si_i^0 and Si_i^{++}) because there is no difference between the charge states in the number of unpaired electron spins. However, $g=2$ for the interstitial pair B_i^+ and B_i^0 because B_i^0 contains an extra unpaired spin compared to B_i^+.

III. RESULTS AND DISCUSSION

Simulations were run for the following ionization transitions treated in the literature as discussed above: $B_i(+/0)$, $B_i(+/-)$, $Si_i(++/0)$, and $Si_i(+/0)$, in which four permutations of the B and Si charge states are possible. Ionization levels were adjusted by trial and error to provide the best fit for each combination. Figures 1–4 show the corresponding simulation results compared to experimental SIMS data for the example case of a spike anneal with a heating rate of 150 °C/s. The figures use this set of experimental data for consistency, although comparisons of the simulations to SIMS profiles taken under other conditions were also made.

Note that the most important feature to fit of the experimental profiles is in regions where the built-in electric field

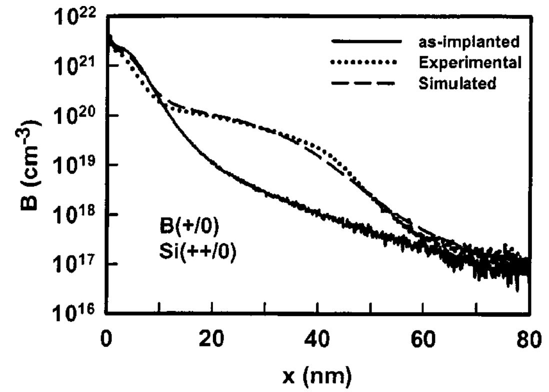

FIG. 1. Example of a FLOOPS profile simulation for $B_i(+/0):Si_i(++/0)$ compared to experimental SIMS data from a spike anneal at 150 °C/s. Fit of the profile slope near the junction at about 50 nm is too shallow.

is high. Although substantial fields can occur near the surface due to electrically active states there by implantation,[7,8] the spatial extent of these fields (~1 nm) is small compared to the length scale of the profiles shown in Figs. 1–4. The other substantial fields in these figures occur down near the junction (where the total concentration of boron reaches 10^{18} cm^{-3}, near $x=50$ nm). The electric field in this region points toward the surface, and opposes the diffusive motion of positively charged species deeper into the bulk. Such effects have been well known for many years.[32] The slope of the simulated profiles reflects how effectively the field opposes this motion, and is quite sensitive to the charge states of the interstitials. The junction depth itself depends upon the charge states as well, but also depends sensitively on certain other parameters in the simulation model such as the activation energy for diffusion of boron interstitials. (Formal sensitivity analysis[14] shows that the diffusivity of silicon interstitials exerts very little effect on the junction depth.) The slopes of the profiles depend much less strongly upon these parameters, and therefore provides a more reliable test of the charge states alone.

Inspection of the figures (and of related data at different heating rates, not shown) shows that the combinations including $B_i(+/0)$ tend to intersect the experimental profiles with a slope that is too shallow near the junction. The charge state on Si_i has no appreciable effect on the profiles with

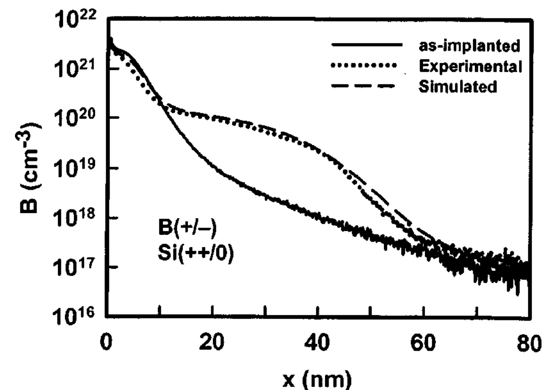

FIG. 2. Comparison of simulation to experiment for $B_i(+/-):Si_i(++/0)$. Both slope and junction depth are fit better with this combination of charge states than the other combinations.

Downloaded 07 Aug 2007 to 130.126.226.215. Redistribution subject to AIP license or copyright, see http://jap.aip.org/jap/copyright.jsp

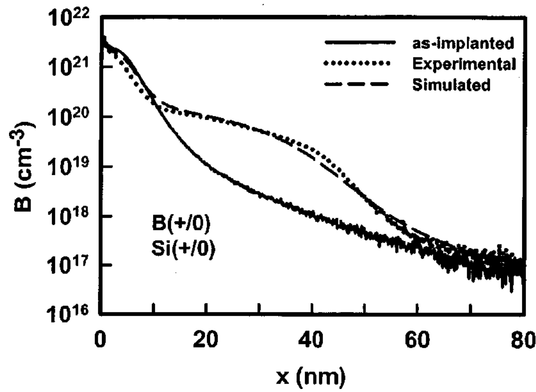

FIG. 3. Profile simulation for $B_i(+/0):Si_i(+/0)$. Results are nearly identical to those of Fig. 1, with $B_i(+/0):Si_i(++/0)$.

$B_i(+/0)$. Combinations including $B_i(+/-)$ do a better job of capturing the slope near the junction, though the charge state on Si_i does exert some influence. Simulations with $Si_i(+/0)$ diffuse further than those with $Si_i(++/0)$, and yield poorer fits—both in terms of the junction depth and the slope near the junction. The $B_i(+/-):Si_i(++/0)$ combination (see Fig. 2) yields the best fit. The corresponding ionization levels $E_{Bi}*$ and $E_{Sii}*$ for the $B_i(+/-):Si_i(++/0)$ pair are 0.33 ± 0.05 and 0.12 ± 0.05 eV above the valence band maximum E_v, respectively. Note that for ease of implementation, and following the spirit of the phenomenology used here, these values were assumed to be independent of temperature in the simulations.

On the basis of Figs. 1–4 and other data sets we have examined, the existence of $B_i(+/0)$ cannot be completely excluded. However, $B_i(+/-)$ provides better fits to the experimental data, especially by the key criterion of slope near the junction. Also, the negative state is necessary to explain near-surface dopant pileup effects observed in other published work,[8] and accords with the negative-U behavior predicted by quantum calculations.

IV. CONCLUSION

This work has attempted to ascertain with greater accuracy the interstitial charge states that are most relevant for boron TED, and has estimated the associated ionization levels. The estimates rely on simulations of experimental diffusion profiles, and therefore the accuracy depends upon the validity of the remaining parameters in the model and on the reliability of SIMS in measuring profile slopes near the junction. The model employed here incorporates parameters derived from mathematically rigorous systems-based methods that combine experimental data together with aggregated computational estimates for the parameters found in the literature. Hence, the model has a greater likelihood of accuracy than alternative *ad hoc* approaches. SIMS suffers from well-known limitations in measuring dopant profiles, although dopant slopes near the junction under the conditions of our experiments probably suffer less than other metrics of profile shape. Experiments at different maximum temperatures might help if the range of maximum temperatures were sufficiently large to ensure that the Fermi level crosses one of the ionization levels, so that different charge states could be sampled experimentally. However, the strong temperature dependence of profile spreading acts to limit that range, so the chance of such a crossing is modest.

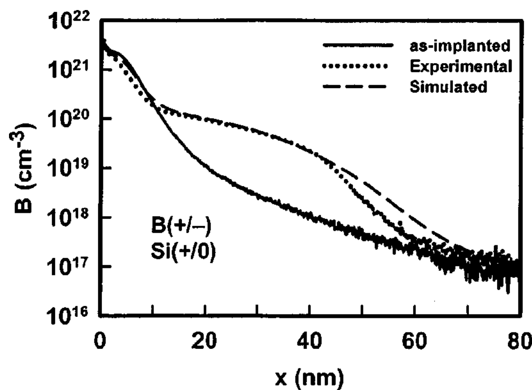

FIG. 4. Profile simulation for $B_i(+/-):Si_i(+/0)$. Slope and especially junction depth are fit less well than in Fig. 2 with $B_i(+/-):Si_i(++/0)$.

ACKNOWLEDGMENTS

This work was supported by NSF (CTS 98-06329 and CTS 02-03237) and by International Sematech.

[1] R. B. Fair, J. J. Wortman, and J. Liu, J. Electrochem. Soc. **131**, 2387 (1984).
[2] P. M. Fahey, P. B. Griffin, and J. D. Plummer, Rev. Mod. Phys. **61**, 289 (1989), and references within.
[3] P. A. Stolk *et al.*, J. Appl. Phys. **81**, 6031 (1997), and references within.
[4] G. Mannino *et al.*, Appl. Phys. Lett. **78**, 889 (2001).
[5] R. B. Fair, *Rapid Thermal Processing* (Academic, San Diego, 1993).
[6] M. McEllistrem, G. Haase, D. Chen, and R. J. Hamers, Phys. Rev. Lett. **70**, 2471 (1993).
[7] K. Dev, M. Y. L. Jung, R. Gunawan, R. D. Braatz, and E. G. Seebauer, Phys. Rev. B **67**, 035311 (2003).
[8] M. Y. L. Jung, R. Gunawan, R. D. Braatz, and E. G. Seebauer, J. Appl. Phys. **95**, 1134 (2004).
[9] S. C. Jain, W. Schoenmaker, R. Lindsay, P. A. Stolk, S. Decoutere, M. Willander, and H. E. Maes, J. Appl. Phys. **91**, 8919 (2002), and references within.
[10] D. Shaw and A. L. J. Wells, Br. J. Appl. Phys. **17**, 999 (1966).
[11] R. B. Fair, J. Electrochem. Soc. **137**, 667 (1990).
[12] M. Y. L. Jung, R. Gunawan, R. D. Braatz, and E. G. Seebauer, AIChE J. **50**, 3248 (2004).
[13] M. Y. L. Jung, R. Gunawan, R. D. Braatz, and E. G. Seebauer, J. Electrochem. Soc. **151**, G1 (2004).
[14] R. Gunawan, M. Y. L. Jung, R. D. Braatz, and E. G. Seebauer, J. Electrochem. Soc. **150**, G758 (2003).
[15] R. Gunawan, M. Y. L. Jung, E. G. Seebauer, and R. D. Braatz, AIChE J. **49**, 2114 (2003).
[16] M. Y. L. Jung, R. Gunawan, R. D. Braatz, and E. G. Seebauer, J. Electrochem. Soc. **150**, G838 (2003).
[17] See Mark Law, http://www.swamp.tec.ufl.edu.
[18] R. D. Harris, J. L. Newton, and G. D. Watkins, Phys. Rev. Lett. **48**, 1271 (1982), and references within.
[19] M. Hakala, M. J. Puska, and R. M. Niemenen, Phys. Rev. B **61**, 8155 (2000).
[20] J. A. Van Vechten and C. D. Thurmond, Phys. Rev. B **14**, 3539 (1976).
[21] J. A. Van Vechten, in *Handbook on Semiconductors*, edited by S. P. Keller (North Holland, New York, 1980), Vol. 3.
[22] K. Dev and E. G. Seebauer, Phys. Rev. B **67**, 035312 (2003).
[23] I. D. Sharp, H. H. Silvestri, H. Bracht, S. P. Nicols, J. W. Beeman, J. L. Hansen, A. Nylandsted Larsen, and E. E. Haller, Mater. Res. Soc. Symp. Proc. **719**, F433-8 (2002); H. Bracht, H. H. Silvestri, I. D. Sharp, S. P. Nicols, J. W. Beeman, J. L. Hansen, A. Nylandsted Larsen, and E. E. Haller, in *Proc. of the 26th Int. Conf. on the Physics of Semiconductors* (ICPS-26), Edinburgh, July 29–August 2, 2002, paper C3.8.

Downloaded 07 Aug 2007 to 130.126.226.215. Redistribution subject to AIP license or copyright, see http://jap.aip.org/jap/copyright.jsp

[24]M. Uematsu, J. Appl. Phys. **82**, 2228 (1997).
[25]W.-C. Lee, S.-G. Lee, and K. J. Chang, J. Phys.: Condens. Matter **10**, 995 (1998).
[26]Y. Bar-Yam and J. D. Joannopoulos, Phys. Rev. B **30**, 2216 (1984).
[27]P. E. Blochl, E. Smargiassi, R. Car, D. B. Laks, W. Andreoni, and S. T. Pantelides, Phys. Rev. Lett. **70**, 2435 (1993).
[28]W. A. Harrison, Phys. Rev. B **57**, 9727 (1998).
[29]J. Zhu, Comput. Mater. Sci. **12**, 309 (1998).
[30]For a review, see D. V. Lang, Annu. Rev. Mater. Sci. **12**, 377 (1982).
[31]P. T. Landsberg, *Recombination in Semiconductors* (New York, Cambridge, 1991).
[32]D. Shaw and A. L. J. Wells, Br. J. Appl. Phys. **17**, 999 (1966).

Downloaded 07 Aug 2007 to 130.126.226.215. Redistribution subject to AIP license or copyright, see http://jap.aip.org/jap/copyright.jsp